Polymer 50 (2009) 2465–2471

Contents lists available at ScienceDirect

Polymer

journal homepage: www.elsevier.com/locate/polymer

Shear-induced orientation in the crystallization of an isotactic polypropylene nanocomposite

Tongchen Sun [a,b], Fenghua Chen [a], Xia Dong [a,*], Yong Zhou [a,b], Dujin Wang [a], Charles C. Han [a,*]

[a] Beijing National Laboratory for Molecular Sciences, Joint Laboratory of Polymer Science and Materials, State Key Laboratory of Polymer Physics and Chemistry and CAS Key Laboratory of Engineering Plastics, Institute of Chemistry, Chinese Academy of Sciences, Beijing 100190, PR China
[b] Graduate School of the Chinese Academy of Sciences, Beijing 100190, PR China

ARTICLE INFO

Article history:
Received 8 December 2008
Received in revised form
30 March 2009
Accepted 30 March 2009
Available online 9 April 2009

Keywords:
Shear-induced crystallization
Polypropylene nanocomposite
Rheology

ABSTRACT

Isothermal crystallization of isotactic polypropylene (iPP)/organic montmorillonite (OMMT) binary composite under shear field was investigated by in situ polarized optical microscopy, rheometry and transmission electron microscopy. When shear strain was small, shear flow could enhance the crystallization of iPP, and the crystallizing entity was spherulitic in iPP/OMMT composite in which the OMMT content was below the percolation threshold. With shear strain increasing, the orientation extent became stronger and cylindrites and strings of spherulites appeared in these samples. However, for iPP/OMMT composite with OMMT content higher than the percolation threshold, when the shear strain was not big enough to destroy the fillers network in the matrix, the crystallization of iPP was similar with that of the un-sheared sample. When shear strain was large enough, the fillers network was destroyed and clay layers were aligned along the flow direction. There formed oriented crystals including cylindrites and strings of spherulites, which were much smaller in size than those formed in the previous case, because the aligned clay layers acted as heterogeneous nucleation agents to promote crystallization of iPP.

1. Introduction

In recent years, isotactic polypropylene (iPP)/clay nanocomposites have drawn increasing attention in both industrial and academic fields because of their better mechanical and thermal properties compared with the pure polymer [1–7]. Crystallization behaviors could have a very large influence on the ultimate properties of the filled iPP. Many groups reported the crystallization behaviors of iPP in the presence of nano-clay fillers under quiescent conditions [8–15], including the crystal forms variation of iPP and heterogeneous nucleation ability of fillers. But there were seldom studies on the crystallization from melts under shear flow in polypropylene composite [16–20].

Processing of polyolefins such as injection molding, film blowing and fiber spinning always involves the application of flow fields, meanwhile, the flow field profoundly affects the nucleation and crystallization behaviors [21–45]. Also, the shish–kebab structure is usually a predominant feature of the morphology when polymers are crystallized from the melt under shear flow. But the origin of the shish formation remains the subject of much debate even now. Keller and co-workers [22–25] proposed that a coil-stretch transition was necessary for creation of an orientated crystalline structure and not the formation of precursors. According to this theory, the longest chains played the key role for the shish formation, in which only the chains longer than the threshold chain length M^* underwent the coil-stretch transition under specified shear conditions. Janeschitz-Kriegl [26,27] stated that the shish precursors grew from point nuclei orientated in the flow direction and were the initial scaffold for the shish formation. Li and de Jeu [30,31] reported that an unusual smectic phase structure was observed in iPP melt under shear field and proposed a new explanation of preordering before polymer crystallization. Hsiao and co-workers [32–34] reported that the stretched polymer chains longer than M^* could aggregate to form extended chain fibrillar crystals and the remaining coil polymer chains could then crystallize upon the fibrillar crystals in a folded periodic fashion, forming the shish–kebab morphology. However, Kornfield and co-workers [35,36] recently proposed that long chains were not the dominant species in shish although they were important for the formation of shish. Kanaya et al. [40,41] studied the shish–kebab formation in polyethylene under shear flow and they found that the radius of the shish-like structure was in micron scale and believed that the shish was formed from the oriented network of high molecular weight chains. Shear-induced crystallization of pure iPP

* Corresponding authors. Tel.: +86 10 82612841; fax: +86 10 62521519.
E-mail addresses: xiadong@iccas.ac.cn (X. Dong), c.c.han@iccas.ac.cn (C.C. Han).

0032-3861/$ – see front matter © 2009 Elsevier Ltd. All rights reserved.
doi:10.1016/j.polymer.2009.03.048

and iPP/poly(ethylene-*co*-octene) (PEOc) blend was extensively investigated in Han's group recently [42–45]. Shish–kebab structure was observed at low shear rates in the crystallization of iPP, which was also obtained in iPP/PEOc blend at the late stage of phase separation under shear flow. The research results led to the model that the nuclei (shish) came from the oriented and entangled polymer network strands instead of pulled-out long chain bundle.

In this paper, iPP/OMMT composite was subjected to shear flow and the crystallization after cessation of shear was investigated. As it is well known, the internal structure of composite sample is different due to the content of OMMT. When the content of OMMT was higher than the percolation threshold, there formed a three-dimensional filler network in the polymer matrix [5,7]. In this iPP/OMMT composite, the percolation threshold was 2 phr (part per hundred parts of polymer matrix) for this kind of OMMT. Generally, flow field had two main effects on the respective molten matrix and fillers, the first was to deform the polymer network anisotropically along the flow direction, and the second was to orientate the fillers parallel to the flow line. In this work, we will discuss the effect of these two kinds of orientations on the crystal morphology of polypropylene in iPP/OMMT binary composite with different OMMT contents.

2. Experimental section

2.1. Materials and preparation

A commercially available iPP (trade marked as T30s, Yan Shan Petroleum China) with molecular weight (M_w) of 4.0×10^5 g/mol and polydispersity index (M_w/M_n) of 4.7 was used as the matrix material. Maleic anhydride (MA) modified polypropylene (PPgMA) with $M_w = 2.1 \times 10^5$ g/mol, $M_w/M_n = 3.2$ and the content of MA 0.9 wt% was used as the compatibilizer, which was purchased from Chen Guang Co. (Sichuan, China). Sodium montmorillonite with a cation exchange capacity of 68.8 mmol/100 g (RenShou, Sichuan, China) was organically modified through ion-exchanged reaction with dioctadecyl dimethylammonium bromide. Samples were prepared the same way as in the previous work [7]. The blend of iPP/PPgMA with a compositional ratio of 90/10 by weight was used as the base resin. The clay layers were intercalated and partially exfoliated and well dispersed in the polymer matrix. The prepared samples were marked as PPCN*x* for iPP/PPgMA/OMMT nanocomposite (*x* stood for the content of OMMT. The unit of OMMT content was defined as phr (part per hundred parts of iPP/PPgMA)).

2.2. Polarized optical microscopy (POM)

Shear flow experiments were conducted in a Linkam Shear Cell (CSS-450, Linkam Scientific Instruments Ltd, Tadworth, Surrey, UK) with two circular parallel plates. The optical microscopy measurements were carried out with a Nikon (Nikon E600POL) optical microscope and a Nikon (COOLPIX4500) camera. In this study, the steady shear was employed to conduct the shear field. The gap between the windows was set as 20 μm. All of the samples were heated from ambient temperature to 200 °C at a rate of 30 °C/min and held for 10 min to eliminate the thermal and mechanical histories of the samples. The experiment procedure including temperature protocol and shear conditions, is shown in Fig. 1.

2.3. Rheological measurements

The rheological measurements were conducted with an Advanced Rheometric Expansion System (ARES, Rheometric Scientific, NJ) which was a strain-controlled rheometer with a cone-plate fixture (25 mm diameter, 0.1 radian cone angle). Disk samples were prepared by compression molding with 1.2 mm in thickness and 25 mm in diameter. Step rate test experiment was carried out at 200 °C with each sample at a constant shear rate of 2.2 s^{-1}.

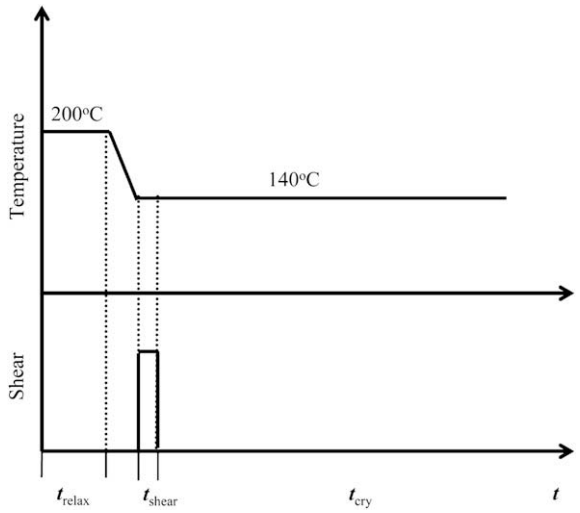

Fig. 1. Schematic description of temperature protocol and shear conditions.

All of the measurements were carried out under a nitrogen atmosphere to avoid oxidative degradation of the specimens.

2.4. Transmission electron microscopy (TEM)

The same shear conditions as those employed in POM experiments were carried out using ARES. After the isothermal crystallization of these samples at 140 °C, the samples were easily peeled off from the fixture in liquid nitrogen. And then these samples were microtomed at −60 °C with a thickness around 100 nm using a Leica EM UC6 ultramicrotome for TEM analysis. The cryosections were collected and directly supported on a copper grid of 300-mesh size. The microscopic study was performed on a JEOL (JEM-2200FS) transmission electron microscope, operating at an accelerating voltage of 200 kV.

3. Results and discussion

3.1. Shear-induced crystallization of PPCN5

Fig. 2 shows the shear time dependence of the characteristic crystal morphologies of PPCN5 during isothermal crystallization at 140 °C after the samples were sheared at a shear rate of 2.2 s^{-1}. When the shear time was less than 20 s, there was no oriented crystal morphology observed in the samples. There was no visible difference between the crystal morphology of PPCN5 under the shear for 10 s and that of PPCN5 without being sheared, which indicated that the effect of shear on crystallization was not obvious in PPCN5 that had been subjected to shear at 2.2 s^{-1} for 10 s. When the shear time was increased to 20 s, although the crystallizing entity was still spherulitic, the number of spherulite was increased dramatically. The evidence of shear on crystallization began to be tangible.

When shear time was longer than 30 s, oriented crystals, including some cylindrites and some strings of spherulites, started to appear. With shear time increased to 60 s and 90 s, the number of oriented crystals was increased greatly, but the size of crystal was decreased obviously. This could be easily explained as the effect of shear field as following: the entangled polymer chain network and

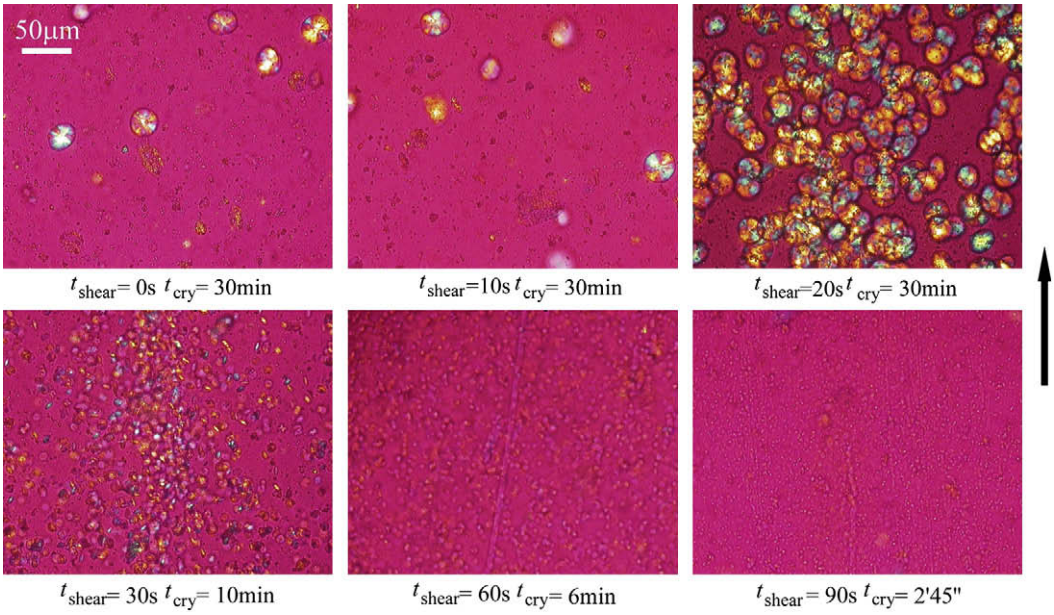

Fig. 2. The characteristic crystal morphologies of PPCN5 during isothermal crystallization at 140 °C after the samples were sheared at a shear rate of 2.2 s^{-1} for different shear times. The arrow indicates the flow direction.

the filler network were both stretched and oriented along the flow direction when shear field was exerted. The strength of the flow could be depicted as the shear strain which was the product of shear rate and shear time. With shear strain increasing, the orientation degree of polymer chain network was increased, the filler network was also deformed and clay layers were aligned along the flow direction in the polymer matrix. The oriented and entangled iPP network strands induced the formation of oriented crystals and the re-dispersed clay layers acted as heterogeneous nucleation agents, which greatly influenced the crystal morphology of iPP and enhanced the number of crystals in the polymer matrix.

From the above description, there was an interesting phenomenon that the shear effect on the crystallization of iPP in PPCN5 was not observed when the shear strain was small (≤2200%). In order to understand this problem, the other two samples (PPCN0 and PPCN1) were chosen to conduct experiments at the same conditions.

3.2. Effect of clay content

Fig. 3 shows the characteristic crystal morphologies of PPCN0, PPCN1 and PPCN5 during isothermal crystallization at 140 °C after being sheared at 2.2 s^{-1} for different shear times. The number of crystal and the degree of orientation in PPCN0 and PPCN1 were greatly enhanced with the increase of shear time as well. Although the crystallizing entities of PPCN0 and PPCN1 were spherulitic after the shear flow for 10 s was applied, the numbers of spherulite in both samples at this condition were larger than those during quiescent conditions respectively. This indicated that the effect of shear flow on crystallization of iPP was tangible in PPCN0 and PPCN1. The further increase of shear time to 30 s induced the formation of cylindrites and strings of spherulite in all of these three samples. When the shear time was increased to 90 s, more cylindrites were formed and the number of spherulite was much larger and the size of crystal became smaller. From the above description, it was clear that shear effect on crystallization of iPP was tangible in PPCN0 and PPCN1 at shear time of 10 s and shear rate of 2.2 s^{-1} while it was not in PPCN5. So it was speculated that shear-induced crystallization of iPP in polypropylene composite had relationship with the content of fillers.

Here the crystal morphologies of these three samples under the same shear conditions were compared. Firstly, when there was no shear exerted, the crystallizing entity was spherulitic and the number of spherulite was increased with the increase of the OMMT content. Secondly, when the shear time was not less than 30 s at 2.2 s^{-1}, it could be observed the formation of cylindrites and strings of spherulite in these three samples. Although the crystal morphology was similar in these three samples at the same shear condition, the number of crystal was greatly enhanced with the increase of OMMT content. The difference of spherulite number among these three samples was caused by the heterogeneous nucleation effect of OMMT layers.

However, when shear time was 10 s at 2.2 s^{-1}, the spherulite number in PPCN0 and that in PPCN1 was larger than that in PPCN5, respectively. Due to the differences in the nucleation rates of these three samples, the crystal growth time was very different. Therefore, we could not compare the size of spherulites in PPCN5 with those in PPCN0 and PPCN1 in this set of figures. As it is well known, there is the effect of heterogeneous nucleation with the addition of OMMT layers. But the number of crystal in PPCN5 was the smallest at this shear condition. From the above analysis, we knew that shear effect on crystallization was tangible in PPCN0 and PPCN1 but it was not in PPCN5 when shear strain was less than 2200%. The only difference among these three samples was the content of OMMT. There was no three-dimensional filler network in PPCN0 and PPCN1 while there was one in PPCN5 because that the content of OMMT was higher than the percolation threshold [5,7]. The filler network limited the motion of polymer chains and helped to increase the structural stability of polymer matrix [7]. In other words, until this network is broken by a large shear strain (such as shear strain larger than 2200%), a distorted network can be quickly relaxed and restored after the cessation of shear. So the shear effect on crystallization was not tangible when PPCN5 was sheared at 2.2 s^{-1} for 10 s or less and only the heterogeneous nucleation effect of OMMT layers was obvious.

When the shear strain was large enough for the filler network to be destroyed in PPCN5, such as the shear time for 30 s, 60 s and 90 s at shear rate of 2.2 s^{-1} shown in Fig. 2, the filler network was destroyed and clay layers were re-dispersed in the polymer matrix.

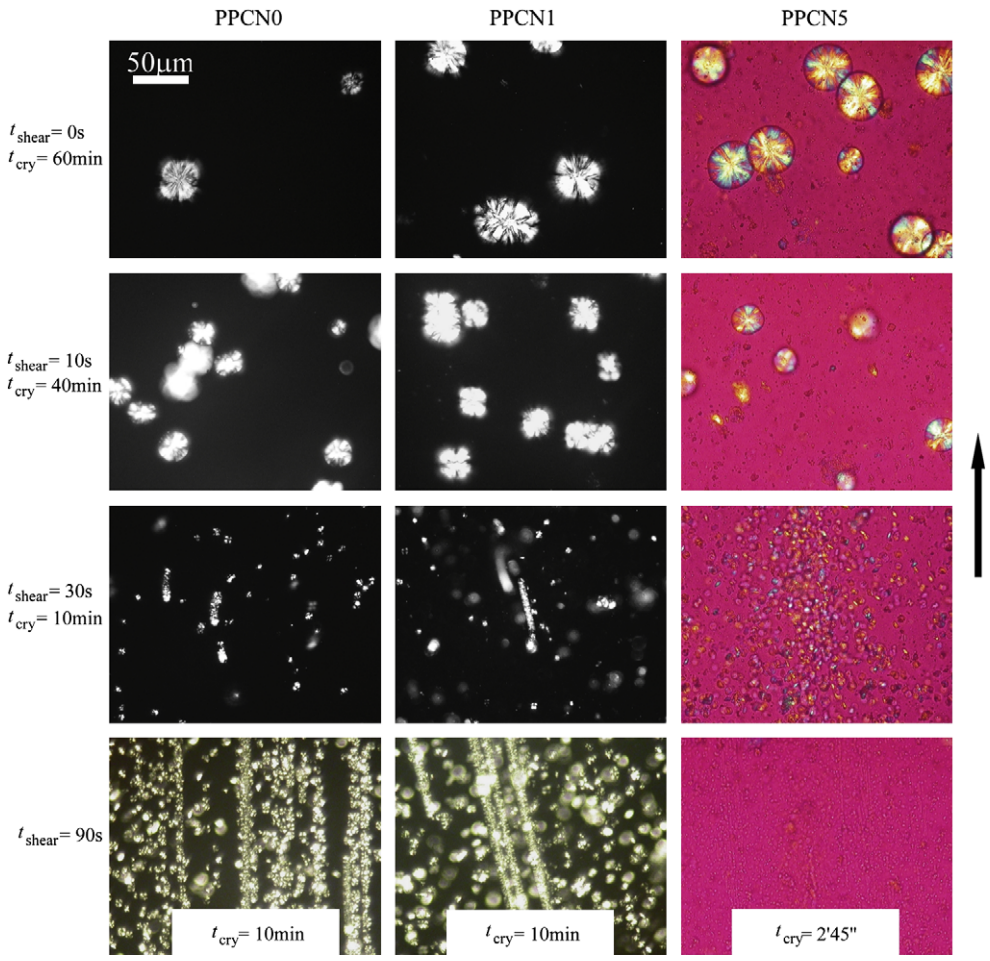

Fig. 3. The characteristic crystal morphologies of PPCN0, PPCN1 and PPCN5 during isothermal crystallization at 140 °C after being sheared at 2.2 s^{-1} for different shear times. The arrow indicates the flow direction.

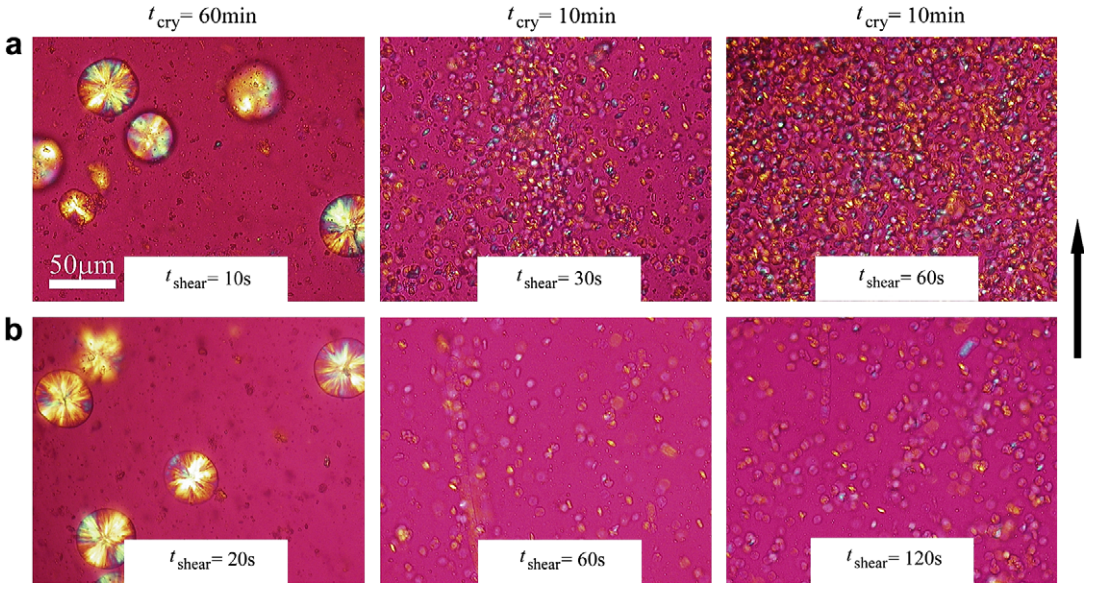

Fig. 4. The crystal morphologies of PPCN5 during isothermal crystallization at 140 °C after being sheared at 2.2 s^{-1} (row a) and 1.1 s^{-1} (row b) for different times. The arrow indicates the flow direction.

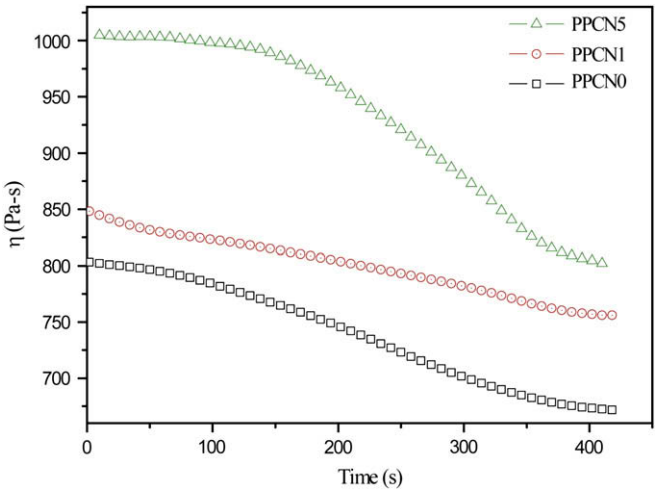

Fig. 5. Viscosity of PPCN0, PPCN1 and PPCN5 as a function of shear time at a shear rate of 2.2 s^{-1} at 200 °C.

In this case, more surface area of clay layers was exposed to polymer chains and available as heterogeneous nucleation sites for polymers. Besides, shear could also enhance the nucleation of polypropylene due to the shear-induced chain alignment. So the number of crystals in PPCN5 was greatly increased with the increase of shear strain.

Form the above analysis, we found the interesting phenomenon that shear effect on crystallization in PPCN5 was not tangible when shear strain was less than 2200% while it was in PPCN0 and PPCN1. It was speculated that this was caused by the formation of the three-dimensional filler network in PPCN5.

3.3. Effect of the shear rates

Fig. 4 shows the crystal morphologies of PPCN5 during isothermal crystallization at 140 °C after being sheared at 2.2 s^{-1} (row (a)) and 1.1 s^{-1} (row (b)) for different times. The image at row (a) and the one at row (b) corresponded to the same shear strain. The crystal morphology of PPCN5 at row (b) was similar with that at row (a), although the number of crystal was a little different. The difference of crystal number between the upper image and the lower one became larger with the increase of shear time. This difference was caused by the difference of the shear time with the same shear strain. During the shear process, it was a competition between shear alignment and molecular relaxation. In other words, there was relaxation of polymer chains and clay layers during the shear. This meant that shear effect on crystallization was more obvious at higher shear rate and shorter shear time, which had been reported by Hsiao et al. [33]. Since the crystal morphology of PPCN5 at row (a) was similar with that at row (b) at the same shear strain, it could be concluded that shear strain was an important factor affecting the crystallization of polymer.

The internal structure of iPP/OMMT composite was also determined rheologically. Shear viscosity of the sample was measured with a fixed shear rate of 2.2 s^{-1} at 200 °C to deduce the internal structure as shown in Fig. 5. Apparently, the viscosity of PPCN0 dropped quickly as shear time going on, so was that of PPCN1. The drop of viscosity indicated that polymer network was oriented and polymer chains (strands) were aligned parallel to flow direction. At

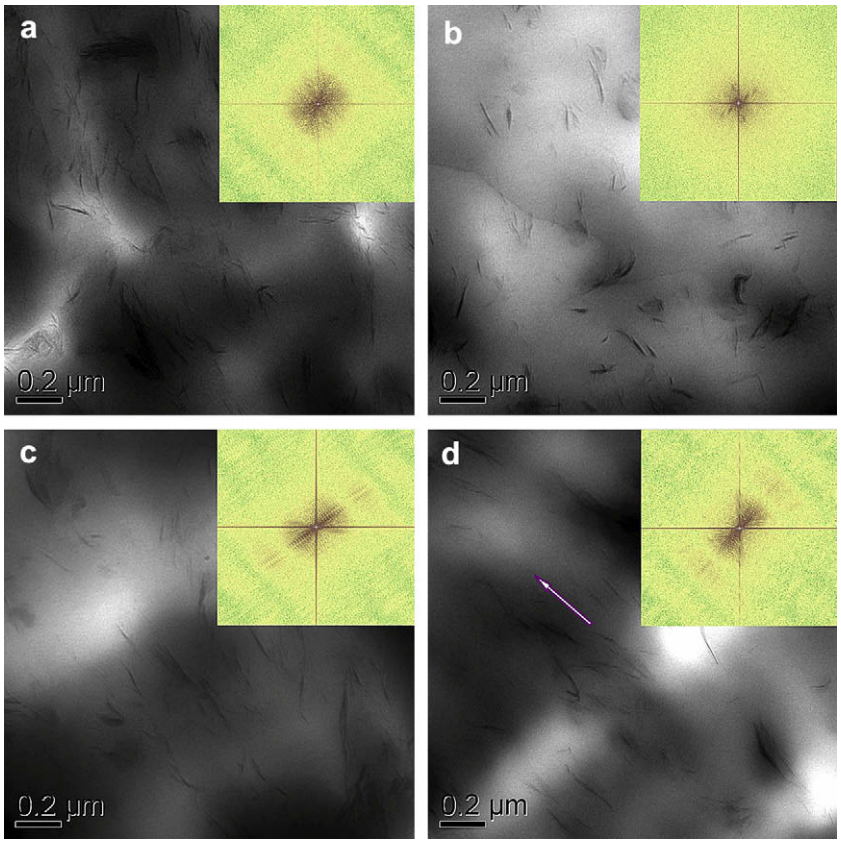

Fig. 6. TEM images of PPCN5 after isothermal crystallization at 140 °C at the shear rate of 2.2 s^{-1} for different shear times: (a) 0 s; (b) 10 s; (c) 30 s; (d) 90 s. The insets are the Fast Fourier Transform (FFT) images of TEM images, respectively. The arrow indicates the flow direction.

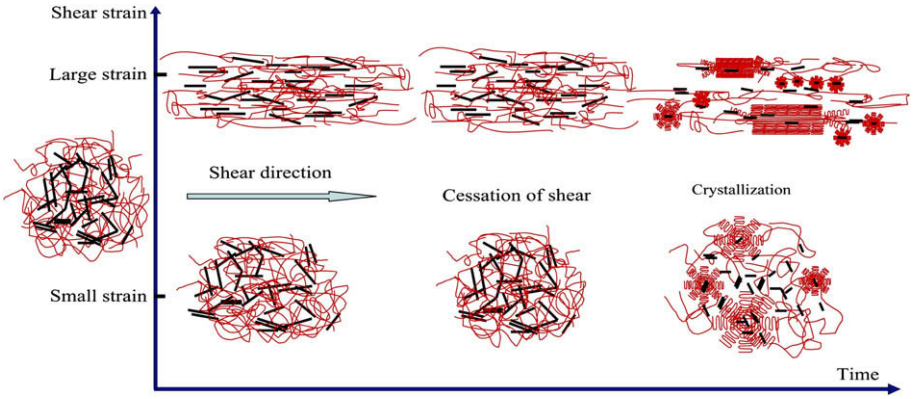

Fig. 7. The proposed model for the shear-induced crystallization of iPP/OMMT composite with OMMT content higher than the percolation threshold.

the first tens of seconds, the viscosity of PPCN1 dropped more quickly than that of PPCN0. This was because that the small amount of clay layer acted as a plasticizer in the polymer matrix instead of forming a three-dimensional filler network [5].

But for PPCN5, the shear viscosity vs. shear time curve showed a plateau at the first tens of seconds, which meant that the internal structure was not changed greatly. And then the viscosity dropped gradually. This indicated that the three-dimensional filler network played a great role in the structural stability of polymer matrix at the beginning of the shear process. When shear flow was applied at the beginning, shear force deformed the polymer network and the filler network. The compact filler network limited the motion of polymer chains. The filler network started to break up as shear time increased (so was shear strain), then the network was deformed and destroyed and the viscosity started to drop.

3.4. Internal structure of PPCN5 after isothermal crystallization under shear field

Fig. 6 shows the TEM images of PPCN5 after isothermal crystallization at 140 °C and at the shear rate of 2.2 s^{-1} for different shear times. The clay layers were mainly exfoliated and partially intercalated and well dispersed in the polymer matrix in Fig. 6. In order to know the statistical information of the TEM image, it was treated through Fast Fourier Transform (FFT) after making binary in Scion Image (Scion Image 4.02Beta) and added as the inset in each panel correspondingly. There was no special information in the FFT image of the un-sheared sample, so was that of the sample in Fig. 6(b). There appeared a streak perpendicular to flow direction in the FFT image when shear time was increased to 30 s and the streak became much stronger with shear time increased to 90 s. The streak showed that there was obvious orientation of clay layers shown in the insets of Fig. 6(c) and (d), which indicated that filler network was orientated and destroyed and most of the clay layers were aligned along flow direction when shear strain was large enough. The orientation degree was most obvious in Fig. 6(d) which showed the TEM image of PPCN5 after being sheared for 90 s. In Fig. 6(b), the dispersion of clay layers was random and there was no orientation of clay layers after PPCN5 was sheared for 10 s. It was similar with Fig. 6(a) which showed the TEM image of un-sheared sample. This was in accord with the previous observation with polarized optical microscope. When PPCN5 sample was sheared at 2.2 s^{-1} for 10 s, the filler network was not destroyed and the fillers were not aligned along flow direction.

Based on the observations and discussion, a model for the aligning mechanism was sketched and proposed to depict the shear-induced crystallization of iPP/OMMT composites with high filler contents as shown in Fig. 7. In iPP/OMMT binary composite with high filler contents, there was a three-dimensional filler network in the polymer matrix. This filler network limited the motion of polymer chains and helped to increase the structural stability of polymer matrix. When shear flow was exerted, the filler network firstly endured the shear force to deform. As the shear strain started to increase as shown in the lower row of Fig. 7, the filler network was deformed, but this deformation could be quickly restored after the cessation of shear. As long as this relaxation time was faster than the growth rate of crystallization, the crystallization of this sample could be just like that of the sample crystallized at quiescent conditions. The crystallizing entity was spherulitic and there were no oriented crystals. This was not observed by Hsiao et al. [19], who reported the crystallization behaviors of iPP/aramid fiber composite under shear field. That may be due to the reason that the shear strain used in their report was relatively large, which was similar with the result shown in the upper row of Fig. 7. If the shear flow was strong as shown in the upper row of Fig. 7, the filler network was destroyed and most of the clay layers were aligned along flow direction and re-dispersed in the polymer matrix. And the polymer network was stretched and oriented along the flow direction, too. So there formed some strings of spherulites and the cylindrites as shown in Fig. 7 (upper row).

4. Conclusion

In this study, crystallization of iPP/OMMT binary composite under shear field was investigated. The crystallization of PPCN5 under shear field was different from that of PPCN0 when shear strain was small. Shear flow could enhance the crystallization of PPCN0 and PPCN1 even though shear strain was small. And the effect of shear on crystallization became stronger with the shear strain increasing. However, the crystallization of PPCN5 was not influenced by shear flow after being sheared at 2.2 s^{-1} for 10 s and the crystallization behavior was similar with that of the un-sheared sample because the filler network in PPCN5 was not destroyed under small shear strain. When shear strain was large enough to destroy the filler network and align the clay layers along the flow direction, then oriented crystals were formed that included not only strings of spherulites but also cylindrites which were occurred from the stretched polymer network strands under shear fields.

Acknowledgements

We would like to thank Dr. Ke Wang and Professor Qiang Fu of Sichuan University for their help to prepare the primary-batch of the sample, and also thank the generous financial support by following grants: National Natural Sciences Foundation of China, Grant No. 20574081.

Reference

[1] Ray SS, Okamoto M. Prog Polym Sci 2003;28:1539.
[2] Kawasumi M, Hasegawa N, Kato M, Usuki A, Okada A. Macromolecules 1997;30:6333.
[3] Giannelis EP. Adv Mater 1996;8:29.
[4] Manias E, Touny A, Wu L, Strawhecker K, Lu B, Chung TC. Chem Mater 2001;13:3516.
[5] Wang K, Liang S, Deng JN, Yang H, Zhang Q, Fu Q, et al. Polymer 2006;47:7131.
[6] Kim DH, Fasulo PD, Rodgers WR, Paul DR. Polymer 2007;48:5308.
[7] Sun TC, Dong X, Du K, Wang K, Fu Q, Han CC. Polymer 2008;49:588.
[8] Saujanya C, Radhakrishnan S. Polymer 2001;42:6723.
[9] Svoboda P, Zeng CC, Wang H, Lee LJ, Tomasko L. J Appl Polym Sci 2002;85:1562.
[10] He JD, Cheung MK, Yang MS, Qi ZN. J Appl Polym Sci 2003;89:3404.
[11] Zheng WG, Lu XH, Toh CL, Zheng TH, He CB. J Polym Sci Part B Polym Phys 2004;42:1810.
[12] Avella M, Cosco S, Volpe GD, Errico ME. Adv Polym Technol 2005;24:132.
[13] Gianelli W, Ferrara G, Camino G, Pellegatti G, Rosenthal J, Trombini RC. Polymer 2005;46:7037.
[14] Yuan Q, Jiang W, An LJ, Misra RDK. Mater Sci Eng A 2006;415:297.
[15] Sun TC, Chen FH, Dong X, Han CC. Polymer 2008;49:2717.
[16] Nowacki R, Monasse B, Piorkowska E, Galeski A, Haudin JM. Polymer 2004;45:4877.
[17] Wang K, Xiao Y, Na B, Tan H, Zhang Q, Fu Q. Polymer 2005;46:9022.
[18] Wang K, Guo M, Zhao DG, Zhang Q, Du RN, Fu Q, et al. Polymer 2006; 47:8374.
[19] Larin B, Marom G, Avila-Orta CA, Somani RH, Hsiao BS. J Appl Polym Sci 2005;98:1113.
[20] Larin B, Avila-Orta CA, Somani RH, Hsiao BS, Marom G. Polymer 2008;49:295.
[21] Pennings AJ, Kiel AM, Kolloid ZZ. Polymer 1965;205:160.
[22] Pope DP, Keller A. Colloid Polym Sci 1978;256:751.
[23] Hill MJ, Barham PJ, Keller A. Colloid Polym Sci 1980;258:1023.
[24] Keller A, Kolnaar HWH. In: Meijer HEH, editor. Materials science and technology. 1st ed., vol. 18. Weinheim: Wiley-VCH; 1997. p. 189.
[25] Lieberwirth I, Loos J, Petermann J, Keller A. J Polym Sci Part B Polym Phys 2000;38:1183.
[26] Liedauer S, Eder G, Janeschitz-Kriegl H. Int Polym Proc 1995;10:243.
[27] Jerschow P, Janeschitz-Kriegl H. Rheol Acta 1996;35:127.
[28] Varga J, Karger-Kocsis J. J Polym Sci Part B Polym Phys 1996;34:657.
[29] Jay F, Haudin JM, Monasse B. J Mater Sci 1999;34:2089.
[30] Li LB, de Jeu WH. Macromolecules 2003;36:4862.
[31] Li LB, de Jeu WH. Phys Rev Lett 2004;92:075506–1.
[32] Nogales A, Hsiao BS, Somani RH, Srinivas S, Tsou AH, Balta-Calleja FJ, et al. Polymer 2001;42:5247.
[33] Somani RH, Yang L, Hsiao BS, Sun T, Pogodina NV, Lustiger A. Macromolecules 2005;38:1244.
[34] Somani RH, Yang L, Zhu L, Hsiao BS. Polymer 2005;46:8587.
[35] Seki M, Thurman DW, Oberhauser JP, Kornfield JA. Macromolecules 2002;35:2583.
[36] Kimata S, Sakurai T, Nozue Y, Kasahara T, Yamaguchi N, Karino T, et al. Science 2007;316:1014.
[37] Dukovski I, Muthukumar M. J Chem Phys 2003;118:6648.
[38] Elmoumni A, Gonzalez-Ruiz RA, Coughlin EB, Winter HH. Macromol Chem Phys 2005;206:125.
[39] Huo H, Jiang SC, An LJ. Polymer 2005;46:11112.
[40] Ogino Y, Fukushima H, Matsuba G, Takahashi N, Nishida K, Kanaya T. Polymer 2006;47:5669.
[41] Kanaya T, Matsuba G, Ogino Y, Nishida K, Shimizu HM, Shinohara T, et al. Macromolecules 2007;40:3650.
[42] Zhang CG, Hu HQ, Wang DJ, Yan SK, Han CC. Polymer 2005;46:8157.
[43] Zhang CG, Hu HQ, Wang XH, Yao YH, Dong X, Wang DJ, et al. Polymer 2007;48:1105.
[44] Meng K, Dong X, Zhang XH, Zhang CG, Han CC. Macromol Rapid Commun 2006;27:1677.
[45] Meng K, Dong X, Hong S, Wang X, Cheng H, Han CC. J Chem Phys 2008;128:024906.